

## Supporting Information

### Interconnected honeycomb-like porous carbon derived from plane tree fluff for high performance supercapacitors

Yunqiang Zhang <sup>a</sup>, Xuan Liu <sup>b</sup>, Shulan Wang <sup>a,\*</sup>, Shixue Dou <sup>c,\*</sup>, Li Li <sup>d,\*</sup>

<sup>a</sup> *Department of Chemistry, School of Science, Northeastern University, Shenyang, 110819, China.*

<sup>b</sup> *Department of Materials Science and Engineering, Carnegie Mellon University, Pittsburgh, PA, 15213, USA.*

<sup>c</sup> *Institute for Superconducting and Electronic Materials, University of Wollongong, Wollongong, NSW 2522, Australia.*

<sup>d</sup> *Department of Materials Science and Engineering, Cornell University, Ithaca, NY, 14850, USA.*

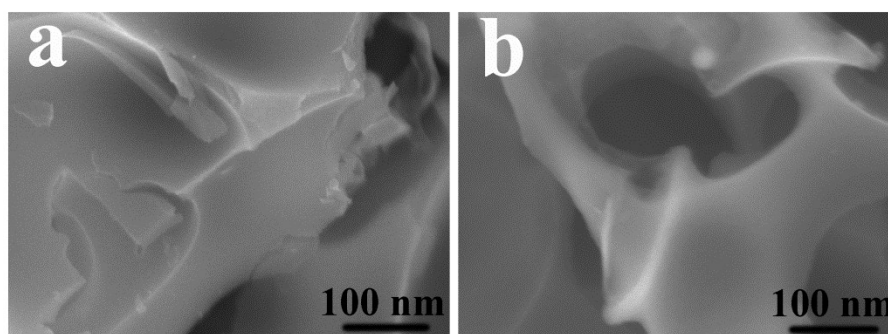


**Figure S1** SEM images of (a) HAC-800 and (b) IHPC-800.

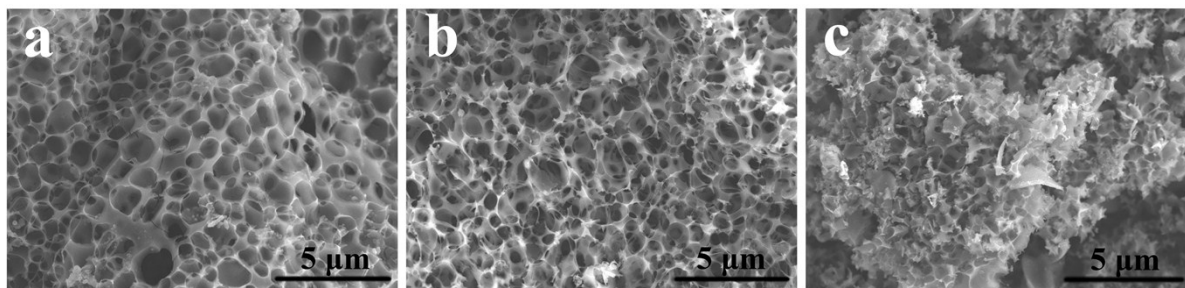


**Figure S2** SEM images of (a) IHPC-700, (b) IHPC-800, and (c) IHPC-900.

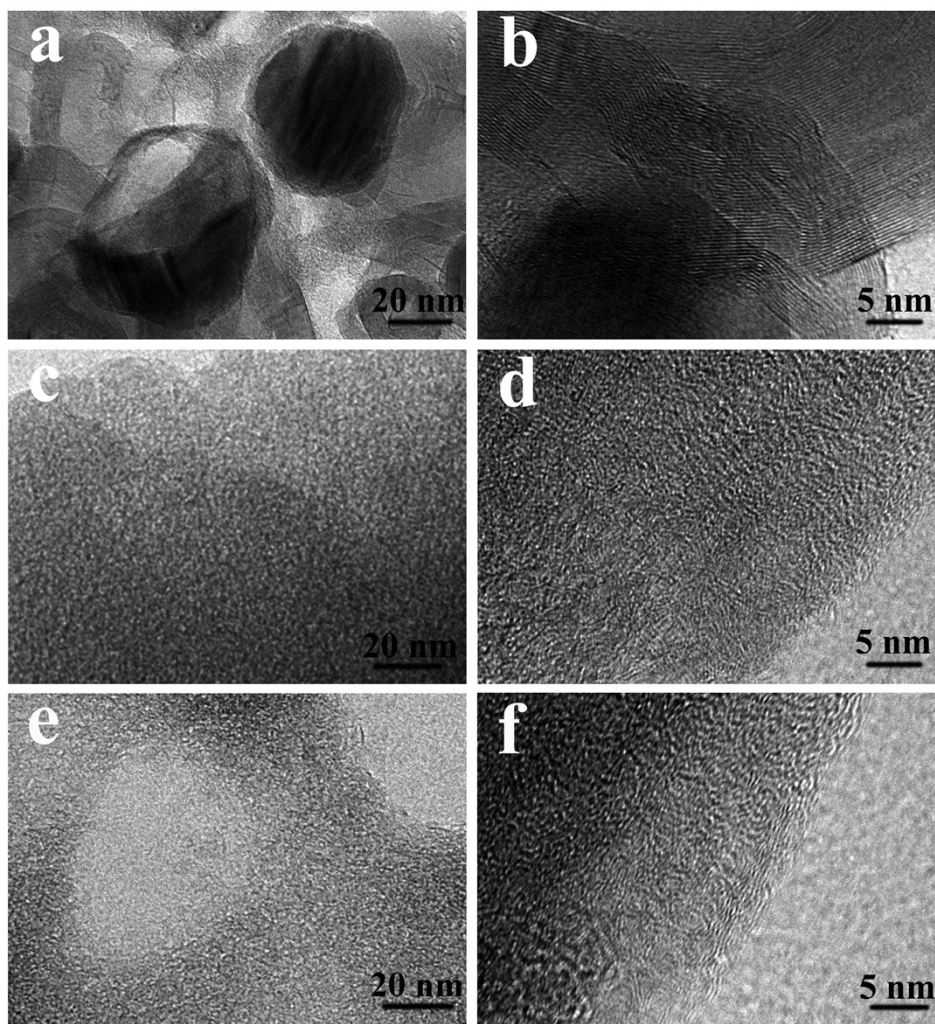


**Figure S3** High-resolution TEM images of (a, b) CT-800 without a post-etching process with HCl, (c, d) HAC-800, and (e, f) IHPC-800.

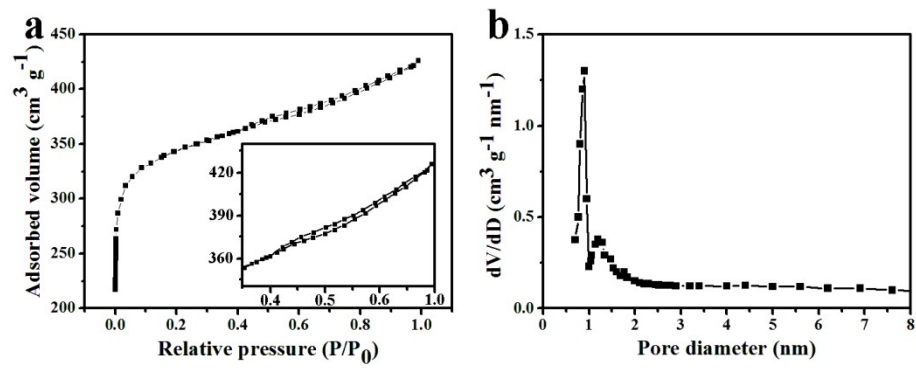


**Figure S4** (a) N<sub>2</sub> adsorption and desorption isotherm, with an enlargement of the hysteresis loop as inset, and (b) pore size distribution of IHPC-800.

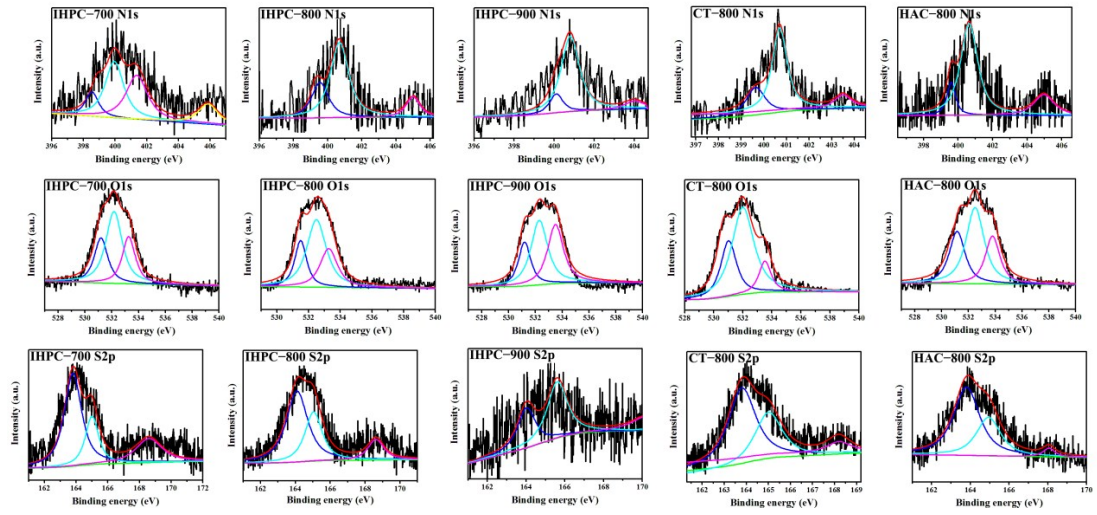


**Figure S5** High-resolution XPS scans for N1s, O1s, and S2p of the IHPC materials and control samples.

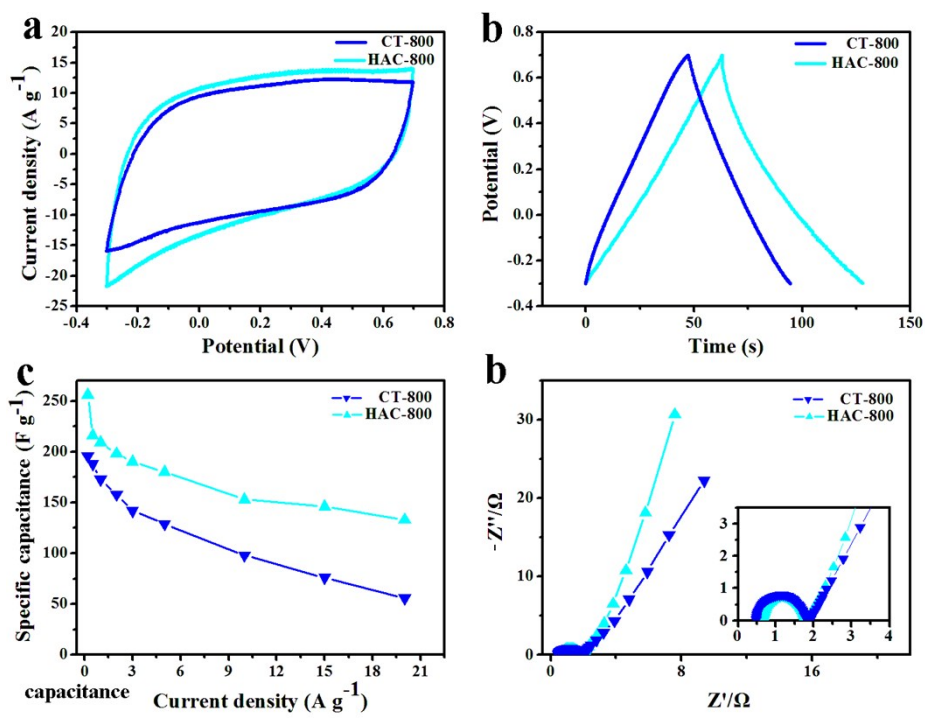


**Figure S6** Electrochemical performance of CT-800 and HAC-800 in a three-electrode cell in 2 M H<sub>2</sub>SO<sub>4</sub>. (a) CV curves at 50 mV s<sup>-1</sup>. (b) GCD curves at the current density of 3 A g<sup>-1</sup>. (c) Specific capacitance at different current densities. (d) Nyquist plots, with an enlargement of the high frequency region as inset.

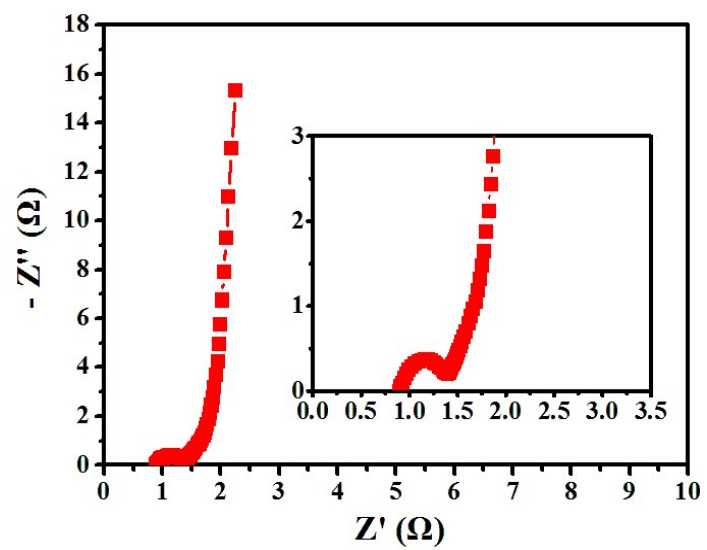


**Figure S7** Nyquist plot of IHPC-800 based symmetrical SCs in 2 M H<sub>2</sub>SO<sub>4</sub>, with an enlargement of the high frequency region as inset.

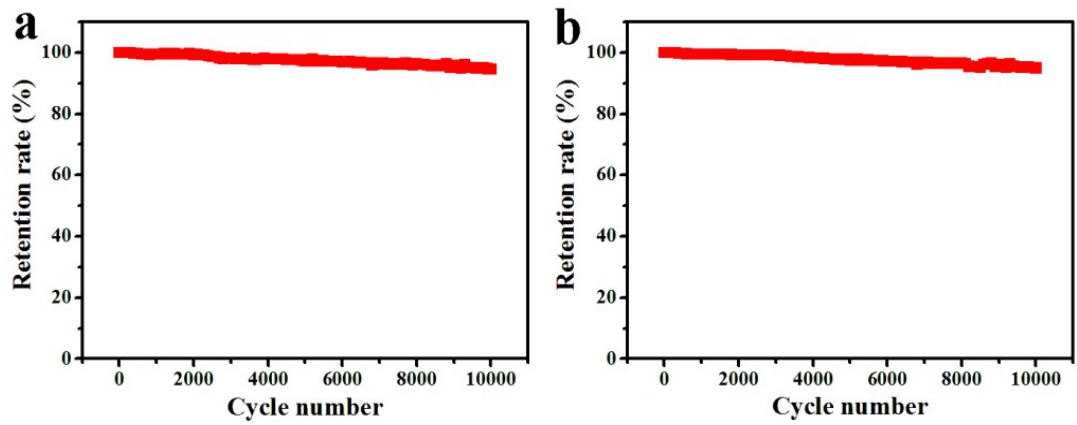


**Figure S8** Cycling stability of HIPC-800 based symmetrical SCs (a) in 2 M  $\text{H}_2\text{SO}_4$  ( $5 \text{ A g}^{-1}$ ) and (b) in 1 M  $\text{LiPF}_6$  in EC/DEC ( $2 \text{ A g}^{-1}$ ).

**Table S1** Comparison of the electrochemical performance of the as-prepared samples with other bio-derived carbon materials from recent references.

Precursor	$C_g$ ( $F\ g^{-1}$ )	Current density ( $A\ g^{-1}$ )	Current density ( $A\ g^{-1}$ )/cycle number/ $C_g$ retention (%)	References
Willow catkin	285	1	5/10000/98	[S1]
Human hair	340	1	2/20000/98	[S2]
Seed shell	329	1	-----	[S3]
Banana peel	206	1	10/1000/98.3	[S4]
Banana fibers	74	0.5	0.5/500/89	[S5]
Pomelo peel	342	0.2	10/1000/98	[S6]
IHPC-700	410; 325	0.2; 1	10/10000/96.10	This work
IHPC-800	493; 370	0.2; 1	10/10000/96.01	This work
IHPC-900	395; 306	0.2; 1	10/10000/97.30	This work
CT-800	196; 173	0.2; 1	10 /10000/97.02	This work
HAC-800	256; 209	0.2; 1	10/10000/95.20	This work

**Table S2** Equivalent series resistance ( $R_s$ ) and charge transfer resistance ( $R_{ct}$ ) of as-prepared samples in three-electrode cell.

Samples	$R_s$ ( $\Omega$ )	$R_{ct}$ ( $\Omega$ )
IHPC-700	0.56	0.61
IHPC-800	0.43	0.42
IHPC-900	0.45	0.76
CT-800	0.49	1.30
HAC-800	0.68	1.11

## References

- [S1] Y. Li, G. Wang, T. Wei, Z. Fan and P. Yan, *Nano Energy*, 2016, **19**, 165-175.
- [S2] W. Qian, F. Sun, Y. Xu, L. Qiu, C. Liu, S. Wang and F. Yan, *Energy Environ. Sci.*, 2014, **7**, 379-386.
- [S3] A. Elmouwahidi, Z. Zapata-Benabithé, F. Carrasco-Marín and C. Moreno-Castilla, *Bioresour. Technol.*, 2012, **111**, 185-190.
- [S4] Y. K. Lv, L. Gan, M. Liu, W. Xiong, Z. Xu, D. Zhu and D. Wright, *J. Power Sources*, 2012, **209**, 152-157.
- [S5] V. Subramanian, C. Luo, A. M. Stephan, K. S. Nahm, S. Thomas and B. Q. Wei, *J. Phys. Chem. C*, 2007, **111**, 7527-7531.
- [S6] Q. Liang, L. Ye, Z.-H. Huang, Q. Xu, Y. Bai, F. Kang and Q.-H. Yang, *Nanoscale*, 2014, **6**, 13831-13837.